Sustainable synthesis of eucalyptus globulus – titanium-magnesium nano composite ('EuTiMg NC') for the photocatalytic degradation of methylene blue

Satti Amrutha[1*], *Nilikonda* Dinesh[1], *Yarlagadda* Madhuri[1], *Gade* Naveen Reddy[1], *Venkata* Rao Poiba[2], and *Meena* Vangalapati[3]

[1]B.Tech Student, Department of Chemical Engineering, Auce, Andhra University, AP, India.
[2]Assistant Professor, Department of Chemical Engineering, Auce, Andhra University, AP, India.
[3]Professor, Department of Chemical Engineering, Auce, Andhra University, AP, India.

Abstract. Synthetic dyes that escape into the environment haphazardly endanger both human health and ecosystems. Because of its toxicity and endurance, methylene blue (MB) stands out amongst these dyes as a significant contaminant. Conventional dye removal techniques can entail expensive and energy-intensive procedures. However, there has been a rise in interest recently in investigating sustainable and environmentally suitable substitutes for dye degradation. Because of their availability, affordability, and innate capacity to interact with contaminants, natural materials like leaves have become increasingly attractive options for restoration of the environment. Eucalyptus Globulus blended with titanium and magnesium nanoparticles to yield a novel environmentally friendly composite, 'EuTiMg'. The degradative capacity of the composite against methylene blue, a prevalent pollutant in water, was assessed by a range of analytical methods, such as SEM, TGA, FTIR, and BET analysis. To increase the composite's photocatalytic activity, we also used Response Surface Methodology (RSM) to optimize the synthesis process. According to our research, 'EuTiMg' composite exhibits better pollutant degrading efficiency and is environmentally benign, making it a viable sustainable option for water treatment applications.

Keywords. Methylene Blue, Nano composite, Eucalyptus Globulus, SEM, FTIR, XRD, RSM, Photocatalytic

1 Introduction

Synthetic dyes that escape into the environment haphazardly endanger both human health and ecosystems. Because of its toxicity and endurance, methylene blue (MB) stands out amongst these dyes as a significant contaminant. Conventional dye removal techniques can entail expensive and energy-intensive procedures. However, there has been a rise in interest

[*] Corresponding Author: 320106205008@andhrauniversity.edu.in

recently in investigating sustainable and environmentally suitable substitutes for dye degradation. Because of their availability, affordability, and innate capacity to interact with contaminants, natural materials like leaves have become increasingly attractive options for restoration of the environment.

1.1 Methylene Blue

Dyes are used extensively in a variety of industries around the world, including the food, paper, and cosmetics industries. Because of the ease of synthesis and chemical stability, the majority of these dyes are utilized in the textile industry [1]. Above 7×10^5 tons of coloring are produced annually worldwide, with 60–70% of that amount coming from Azo coloration [2]. But using these artificial dyes has major repercussions on the environment. These industrial aqueous effluents might contain tinctorial effluents, which have the potential to be hazardous or carcinogenic to individuals or animals in addition to being poisonous or harmful to microbial communities [3]. Though it has a wide range of adverse effects, methylene blue has not been identified to be particularly harmful. Inhaling it can result in brief episodes of rapid or labored breathing. Oral swallowing results in burning and increases the risk of gastritis, diarrhea, nausea, and vomiting [4]. This sort of dye can be removed using a variety of physical, chemical, and biological techniques, including membrane filtering, advanced oxidation, ozonation, coagulation, irradiation, coagulation, ion exchange, and electrochemical destruction [5]. However, these technologies' limited ability for adaptation to a broad spectrum of dye wastes and their expensive cost limit their application [6]. Use of photocatalysts has been considered as one of the most promising ways of removing organic compounds from water [7].

1.2 Green Synthesis

Reliable processes including membrane filtration, adsorption on activated carbon, flocculation, and coagulation cannot easily break down dyes. These chemicals' complicated structures and greater stability make it harder to convert them into non-toxic molecules. To get over these challenges, scientists are leaning toward using green synthesized metal oxide nanoparticles (NPs) as a green catalyst to break down organic pollutants [8]. According to the studies conducted by Aoumria Ouldmoumna et al . It was found that each gram of Eucalyptus globulus leaves adsorbed 250mg of Methylene Blue at an optimum pH of 10 [9].

1.2.1 Titanium Di Oxide Nanoparticles

The TiO2 has been most frequently employed as the photocatalyst owing to its cheapness, nontoxicity, and structural stability [10-13]. Although TiO2 is having versatile applications, basic TiO2 will absorb only mid to-high UV light (280 nm to 380 nm) with the band gap energy of 3.2 eV, which is less abundant in sunlight. To increase the photocatalytic efficiency and light absorption capacity to wide range of sunlight, there is a need of visible light absorbing organic compounds to graft with TiO2. Recently numerous photocatalytic works are publishing in research community [14–17].

1.2.3 Magnesium Oxide Nanoparticles

Magnesium oxide (MgO) is a substance that is widely used in many different applications, including catalysis, refractory material in manufacturing, and antibacterial material. With many features such as a broad band gap, great thermal stability, low refractive index, and low dielectric constant, magnesium oxide (MgO) is a useful metal oxide material [18]. The surface characteristics of magnesium oxide nanoparticles (MgO-NPs), such as their surface area, porosity, and surface shape, are critical in determining how effective they are as photocatalysts [19]. The majority of magnesium compounds are significantly less expensive and have good water solubility [20] .

2 Materials and Methods

2.1 Materials:

Eucalyptus globulus leaves, Methylene blue dye, Titanium Dioxide and Magnesium Oxide nano particles

2.2 Apparatus:

UV Light source in a closed chamber along with a mechanically operated stirrer, UV –VIS Spectrophotometer, pH meter, Centrifuge and Glass materials etc.

2.3 Synthesis of Eucalyptus Globulus – Titanium- Magnesium Nano composite ('EuTiMg'):

The leaves of Eucalyptus globulus were gathered from the trees in the vicinity of Juthada village, located in the Visakhapatnam district of Andhra Pradesh, India. To begin the process of preparing the leaf extract, the fresh leaves were cleaned and rinsed with Distilled and tap water to get rid of any dirt, sand, and contaminants. The cleaned leaves were allowed to air dry in the sun until they were completely dry. After being dried, the leaves were ground into a powder and screened to a size of 45 microns. The 45-micron fine leaf powder, TiO2 nanoparticles, and MgO nanoparticles were combined in 5:5:1 ratio respectively by through mixing to prepare EuTiMg.

Fig. 1. (a) Eucalyptus Globulus Leaves

Fig. 1. (b) EuTiMg NC nano composite

2.4 Preparation of dye solution:

By carefully weighing and dissolving 10 mg of Methylene blue in distilled water in 1000 ml (approximately 33.81 oz) volumetric flasks, the dye stock solution at the target concentration of 10 ppm was created independently. After that, an adequate amount of distilled water was added to these stock solutions, and they were gradually diluted to the necessary dye concentration. The sample should be diluted to put the concentration within the measurable range if it is over this range

Fig. 2. 10ppm methylene blue stock solution

2.5 Characterization of EuTiMg NC:

2.5.1 Scanning Electron Microscope-Energy-Dispersive X-ray Spectroscopy (SEM-EDX) Analysis:

SEM (Scanning Electron Microscope) image shown in Fig. 2 clearly indicates the small structures and different sizes of EuTiMg. It provides high resolution and stable probe currents for optimum imaging. The SEM results of EuTiMg NC Scanning Electron Microscope (SEM) show the particle size in 100nm and 200nm in Fig 3 (a) & Fig 3 (b) respectively.

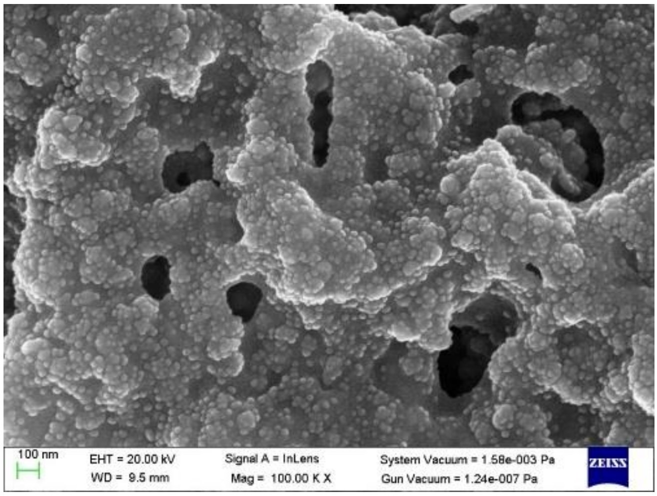

Fig. 3. (a): SEM image of EuTiMg NC in 100nm

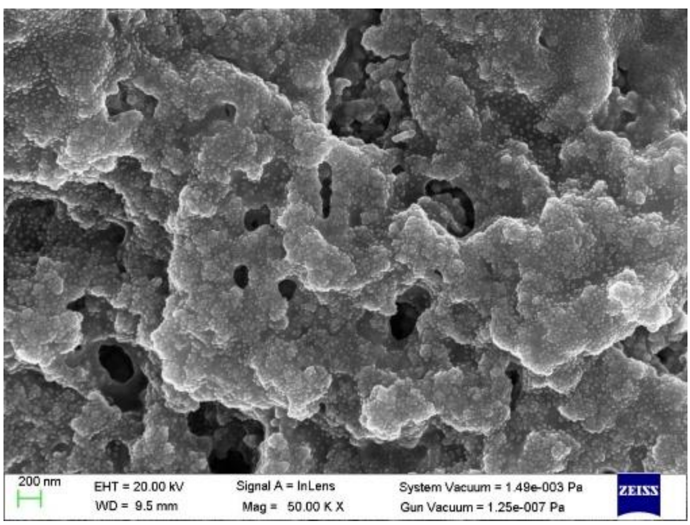

Fig. 3. (b): SEM image of EuTiMg NC in 200nm

2.5.2 Thermogravimetric analysis (TGA) & Differential Thermal Analysis (DTA):

The thermograms were done on the material to study their stability to temperature in order to assess the degassing range for BET analysis and to have information about the carbonization behavior for any subsequent treatment. They presented a first weight loss at low temperature (T < 600˚C) attributed to the elimination of adsorbed water. It corresponds to about 10% for EuTiMg NC and to about 5% for the two other biosorbents. The first mass loss was attributed to the departure of physisorbed water and the second loss at 600˚ C, (600 < T < 650˚C) to the emission of chemisorbed water. The first stage of carbonization occurs in the temperature range of 200–500˚C (70% loss) due to the eradication of volatile material rich in functional groups (lignin, hemicellulose, and cellulose).

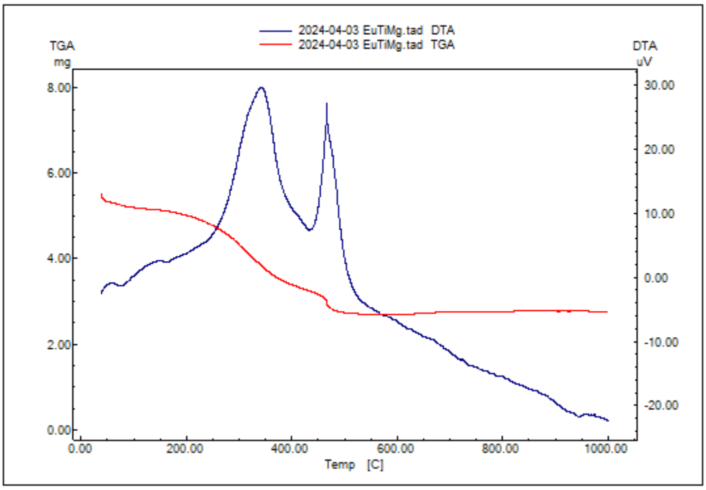

Fig 4. TGA & DTA image of EuTiMg NC

2.5.3 Braunauet-Emmett-Teller (BET) Analysis:

The BET analysis of EuTiMg NC is conducted at the degassing temperature of 343K. It is observed that EuTiMg NC Has a surface area of 4.964 m^2/gm as shown in Fig 4.The BET Single point dynamic flo method of analysis is used to determine the surface area of EuTiMg NC , which is found to be 4.96 m2/g. Nitrogen gas is used as adsorbater ith a partial pressure of 29.98% at a regeeneration temperature and time of of 348k and 120 mins respectively.

IIT Jammu
Chemical Engineering
Jagti Nagrota

BET SINGLEPOINT SURFACE AREA REPORT

Instrument ID	: SMART/SA/01/16-17	Instrument Name	: Surface Area Analyser
Instrument Make	: Smart Instruments	Instrument Model	: SmartSorb 93
Analysis Method	: BET SinglePoint Dynamic Flow Method	Adsorbate Gas	: Nitrogen
Analysis Date	: 06/04/2024	Sample Name	: 6/4/24_EuTiMg
A.R. No.	: 6/4/24_EuTiMg	Start Time	: 16:47:46
Batch. No.	: 1	End Time	: 17:05:54
Empty Tube Weight (gm)	: 24.178	Ambient Temperature (°C)	: 26
Sample + Empty Tube Weight (gm)	: 24.378	N2 Partial Pressure %	: 29.98
Dry Sample + Empty TubeWeight (gm)	: 24.367	Regeneration Temperature (°C)	: 75
Sample weight beforeRegeneration (gm)	: 0.200000	RegenerationTime (min)	: 120
Sample weight after Regeneration(gm)	: 0.189000	NitrogenPurging	: Yes
		Sample Loss (%)	: 5.500000

Analytical Data:	Desorption Count	: 9793	Surface Areain (m^2/gm)	: 4.964091
	Injection Count	: 7257		
	Injected Volume (cc)	: 0.25		

Perform By	: Aditya Shankar Sandupatla	Reviewed By	:
Date	: 06/04/2024 16:47:46	Date	:
		Remarks	:

SmartSorb 1.0 Printed By : Aditya Shankar Sandupatla On 09-04-2024 Page 1 of 1

Fig 5. BET analysis of EuTiMg

2.5.4 Fourier Transform Infrared (FT-IR) analysis:

The functionalities found in the Eucalyptus globulus leaf extract and the characteristics of the TiO2&MgO NPs were identified using FTIR spectroscopy; the resulting spectra are shown in Figure 5. There were notable peaks in the leaf extract spectra at 3500–3100 cm−1, 2400 cm^{-1}, 1600 cm^{-1}, 1020 cm^{-1}, and 600 cm^{-1} The large peak measured between 3500 and 3100 cm^{-1} was ascribed to the frequency of OH stretching. Similarly, the C–H, C=C, and C–O stretching vibrations were responsible for the bands recorded at 2924 cm^{-1}, 1603 cm^{-1}, and 1021 cm^{-1}, respectively [21].The phytochemicals found in the leaf extract, such as glycosides, flavonoids, polyphenols, terpenoids, tannins, carbohydrates, and reducing sugar, are responsible for the peaks that the extract displayed[22].

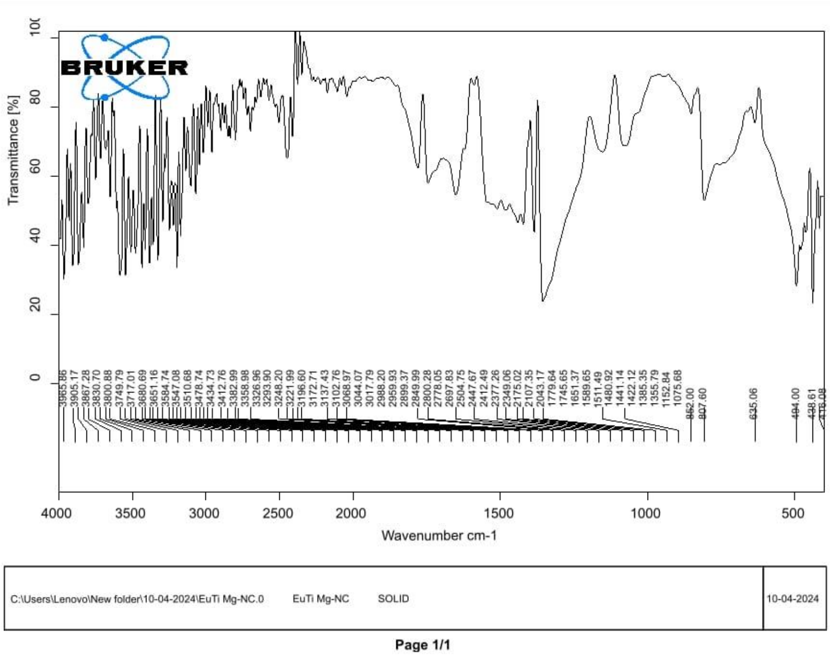

Fig. 6. FT-IR Spectra of EuTiMg

2.5.5 Response Surface Methodology (RSM):

Visualising the statistical significance of the independent factors on the dependent variables will be made easier with the help of the surface contour plots that were developed. The effect of variables including time, temperature, dosage of photo catalyst was observed to determine the extract yield by using the 3D response plot to the experimental data. In this investigation, the extraction duration was adjusted to maximise energy savings and extraction efficiency. An increase in time had a positive impact on the total extraction yield, as shown in Figures 8 and 9. Furthermore, the plots showed that the overall extraction yield stayed mostly constant when the extraction duration was extended beyond 5mins. As seen by Figures 7 and 8, extraction is significantly impacted by temperature. Solvent concentration is another important factor that significantly affects extraction efficiency. When dosage of photo catalyst was examined, a linear effect was observed and proved to be statistically significant. As seen in Figures 7 and 9, this suggests that raising the dosage of photo catalyst leads to an increase in extraction. It was demonstrated that a dosage of photo catalyst of 10mg/100ml was ideal for photocatalytic degradation of methylene blue

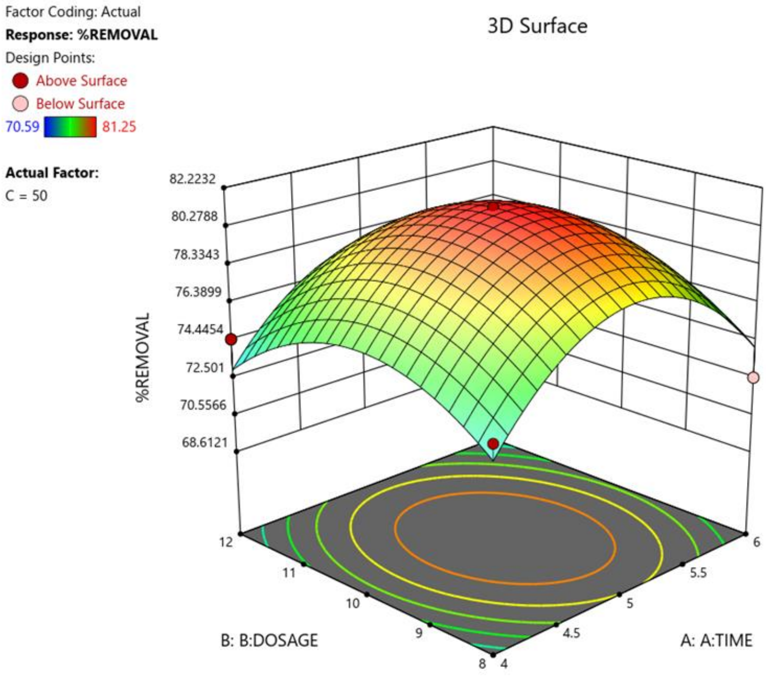

Fig. 7. RSM of EuTiMg (Dosage vs Time)

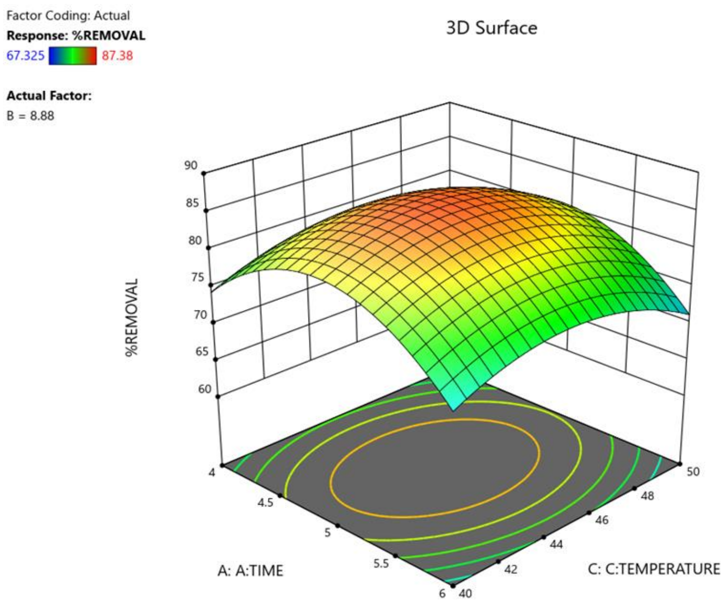

Fig. 8. RSM of EuTiMg NC(Temp vs Time)

https://doi.org/10.1051/e3sconf/202455201042

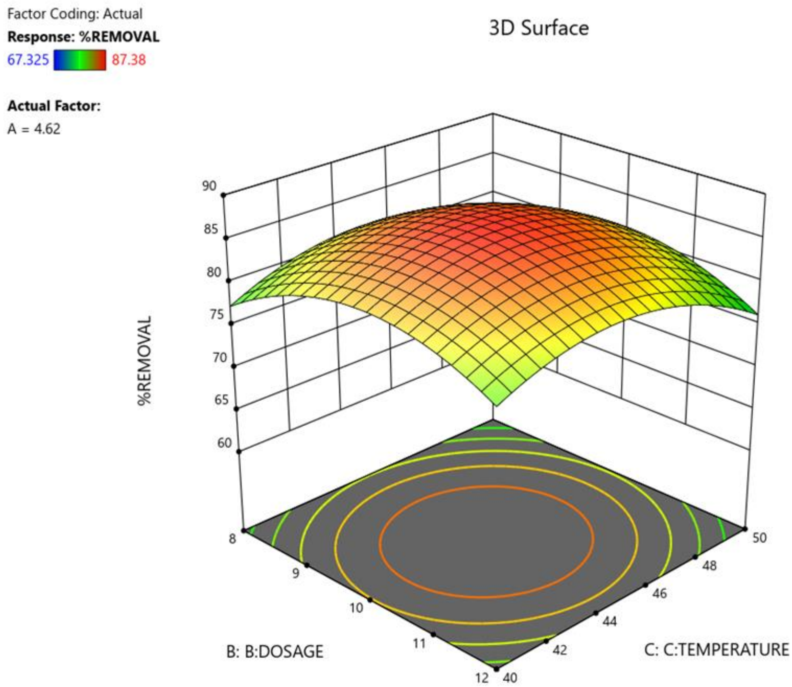

Fig. 9. RSM of EuTiMg NC(Dosage vs Temp)

3 Results and Discussion

3.1. Photocatalytic degradation of Methylene blue:

The degradation of methylene blue has been studied with and without catalyst and UV light, respectively. No catalyst was used, and the concentration of the dye solution did not change much in the absence of a UV light source. Batch tests were therefore carried out in the presence of both photocatalyst and UV light irradiation in order to degrade methylene blue. Using a 100 ml solution of methylene blue in a glass beaker under UV irradiation, the photocatalytic activity of the EuTiMg NCnano composite was assessed in batch experiments at different time intervals, doses, pH levels, starting concentrations, and temperatures. The photocatalytic process caused the blue colour of the solution to progressively fade over time. After the batch investigations, the photocatalyst and Methylene blue solution have been separated from one another using a centrifuge. The centrifuged solutions were analysed with a UV spectrophotometer that was calibrated to 660 nm.

https://doi.org/10.1051/e3sconf/202455201042

Fig. 10. Experimental set up for photo catalyst

3.2. Optimization of process parameters:

3.2.1 Effect of time of the photocatalyst and UV light irradiation:

Using EuTiMg NCas the photocatalyst, photocatalytic degradation tests on synthetic or M.B dye solutions were conducted for varying durations, i.e., from 0 to 30 min at regular intervals of 5 min. As the contact time grew from 0 to 5 minutes, the dye solution's hue diminished. The colour intensity does not vary after five minutes, and even when the contact time is increased, the solution's optical density stays constant. The photocatalyst dose saturation capacity and the UV light source may be the cause of the lack of additional degradation percentage rise. This demonstrates that, as indicated in Fig. 11(a), the ideal contact time was found to be 5 minutes.

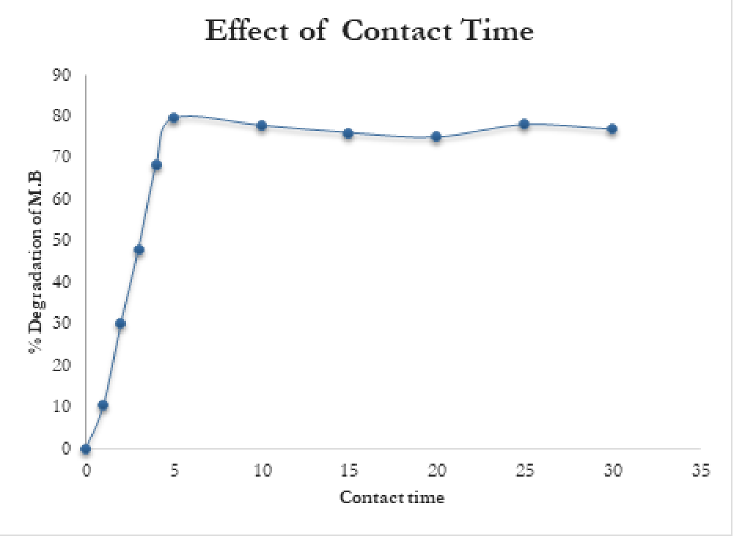

Fig. 11. (a) Effect of Contact time (min) for degradation of M.B dye

(b) Effect of dosage of the photocatalyst:

The degradation process is also significantly influenced by the photocatalyst's dosage. The photocatalytic performance of various photocatalyst dosages, ranging from 2 to 10 mg/100 ml, was investigated. It was found that the dosage of 10 mg/100 ml produced the highest degradation of dye, as illustrated in Fig. 11(b). Additional dosage increases reduced the percentage of degradation because more particles in the dye solution caused it to become opaque and lose its transparency.

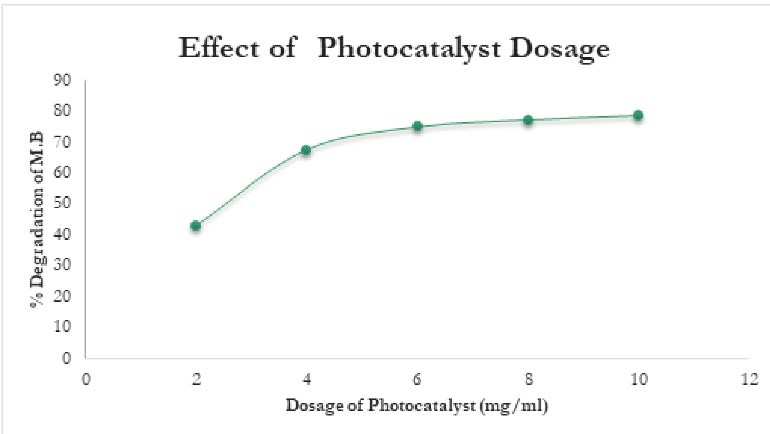

Fig. 11(b) Effect of dosage photocatalyst (mg/100ml) for degradation of M.B dye

(c) Effect of pH of the synthetic M.B dye solution:

The breakdown rate of synthetic M.B dye solution is significantly influenced by its pH. Because of the hydroxyl radicals, there may be notable variations in the degradation as pH fluctuates. Using EuTiMg NCas the photocatalyst, the photocatalytic degradation studies of synthetic M.B dye solution were conducted at various pH values within the range of 7-11, while maintaining a constant dosage and contact time under ideal conditions. From pH 7 to pH 10, dye degradation increased and then decreased as pH rose. The dye degradation reached its maximum (77.12%) at pH 10, as Fig. 11 (c) illustrates.

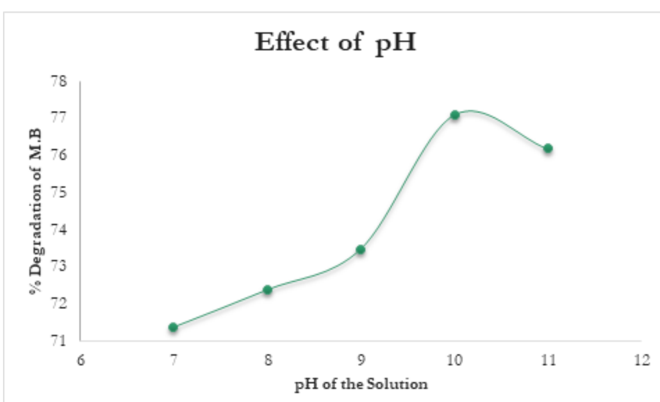

Fig. 11(c) Effect of pH on the degradation of M.B dye

(d) Effect of initial concentration for the degradation of synthetic M.B dye solution:

Keeping temperature, contact time, dose, and pH constant, experiments were conducted on the photocatalytic degradation of synthetic M.B dye solution utilising EuTiMg NCas the photocatalyst, at various starting concentrations. The testes were examined at several starting concentrations between 7 and 11 ppm, as Figure 11(d) illustrates. The dye degradation peaked at 7 ppm.

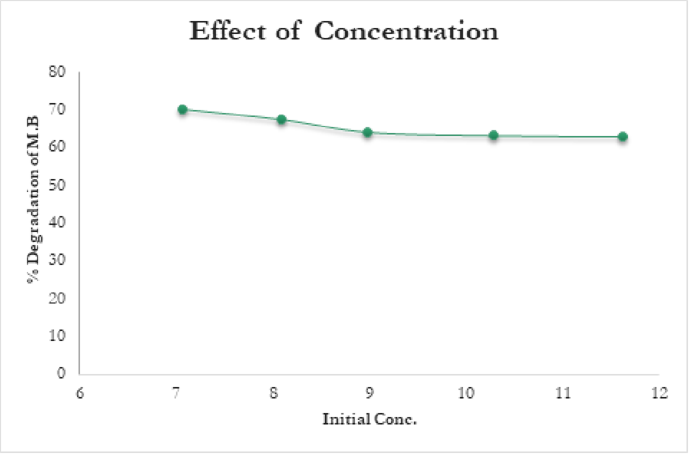

Fig. 11(d) Effect of Concentration on the degradation of M.B dye

(e) Effect of temperature for the degradation of synthetic M.B dye solution:

These tests were all carried out between 308 and 353 K at various temperatures. It was noticed that 79.83% degradation of M.B dye was acquired at the conditions of 7 ppm initial dye concentration and at the temperature of 323K. Figure 11(e) clearly illustrates how the percentage of M.B degradation reached its maximum with an increase in temperature and decrease in initial dye concentration. This is because the dye solution has a lower concentration and because a catalyst's activity coefficient rises with temperature, increasing the rate of reaction and ultimately resulting in maximal degradation.The photocatalyst's catalytic effectiveness is reduced by increasing dye solution concentration, which slows down the reaction and further reduces the percentage of dye degradation. When EuTiMg NCparticles were used in the photocatalytic degradation of methylene blue, the maximum percentage of degradation of 79.82% was achieved under ideal circumstances.

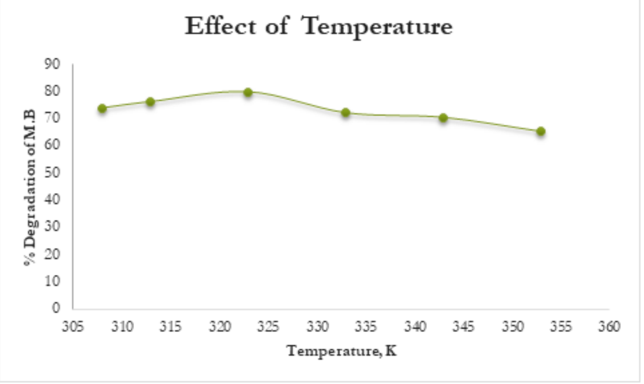

Fig. 11(e) Effect of Temperature on the degradation of M.B dye

3.3 Kinetic study:

The pseudo 1st order and 2nd order kinetics are studied from the graph below and it is observed that reaction fits pseudo second order more promptly. As shown in the Fig.12.

q = Adsorption capacity (milligram of methylene blue dye adsorbed per gram of EuTiMg-Nc) at some time t in minutes

q_e = Equilibrium Adsorption capacity in (mg/g)

$$q = [(C_0 - C_f)/W] * 100 \quad (1)$$

where C_0 and C_f are the initial and final concentrations in ppm respectively

W is the optimum dosage in milligrams of EuTiMg NC per ml of Methylene blue solution.

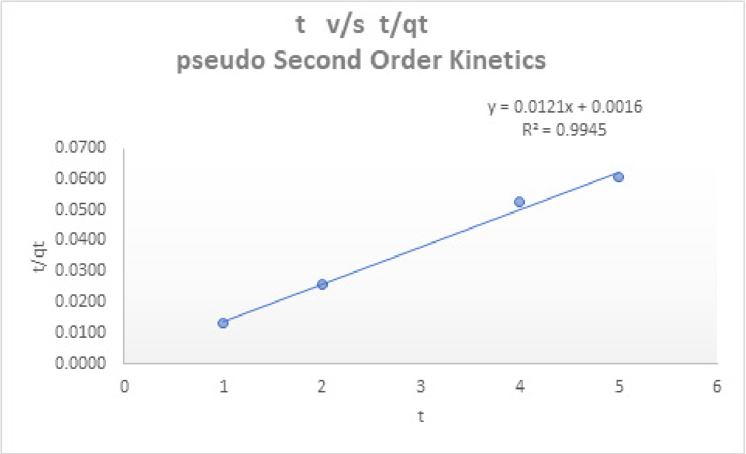

Fig. 12. Pseudo second order kinetics

Calculating the value of rate constant from the line equation of the plot time V/s t/q_t,

The equation obtained was y = 0.0121x + 0.0016

From the equation, positive value of slope gives the rate constant of the reaction process.

Therefore, the rate constant for the degradation reaction of MB dye = 0.091 g/mg.min

Equilibrium adsorption capacity, experimentally q_e (exp) = 82.510 mg/g

Equilibrium adsorption capacity, theoretically q_e = 82.644 mg/g.

3.4. Activation energy and Thermodynamic studies:

Activation energy of the reaction process was determined using Arrehenius equation model, with the plot drawn between ln k and (1/temperature). The plot of ln k Vs 1/T was shown in the figure 13. below.

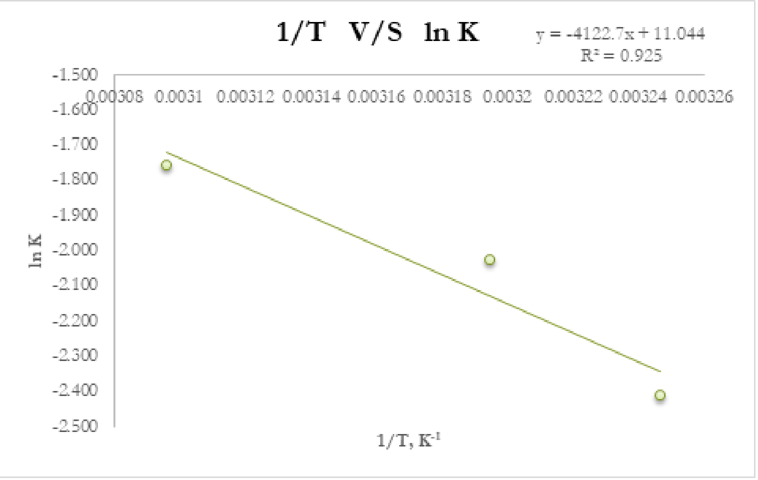

Fig. 13. Plot for determining activation energy, ΔH, ΔS and ΔG for the degradation process using EuTiMg

From the graph shown above the figure 13, comparing the line equation with the Arrhenius law equation, the slope gives the value of activation energy. And when the line equation was compared with the Vant Hoff's equation, the values of ΔH, ΔS and ΔG were determined.

Arrhenius law equation is

$$\ln K = [\,(-E_a/\mathrm{R})\ *(1/T)] + \ln A \tag{2}$$

A line equation obtained from the plot drawn between ln K Vs 1/T for finding the activation energy. The slope of this line equation gives the value of activation energy.

→ Slope = $(-E_a/R)$

$-E_a$ = slope*R

The line equation obtained from the plot was y = -4122.7x + 11.044

Therefore, Ea = -(-4122.7*8.314) =34,276.12 J/mol

From VantHoff equation is

$$\ln K = -\,(\Delta H/\ RT) + (\Delta S/R) \tag{3}$$

The linear equation obtained was y = -4122.7x + 11.044

ΔH = 34.276 KJ/mol

ΔS = 91.819 J/mol K

ΔG = ΔH – TΔS = -RTlnK = 34.276 – (323*91.819) = -29.623 KJ/mol

4 Conclusion

Compared to other widely used traditional approaches, the photocatalytic degradation of methylene blue utilizing the Eucalyptus globulus – titanium – magnesium nano composite

('EuTiMg') offers a straightforward, stable, sustainable, economical, and environmentally beneficial approach. It is evident that a number of variables and optimal catalytic performance settings were the only things influencing EuTiMg's photocatalytic activity. Our research indicates that at an initial concentration of 7ppm and a catalyst dosage of 10 mg/100 ml at a pH of 10 and 323 K, it exhibited a higher rate of photocatalytic degradation of 79.82% during a contact period of 5 minutes. The BET studies show a surface area of 4.964 m^2/gm.

References

1. Bouguettoucha, A.; Chebli, D.; Mekhalef, T.; Noui, A.; Amrane, A. The use of a forest waste biomass, cone of Pinus brutia for the removal of an anionic azo dye Congo red from aqueous medium. Desalin. Water Treat. (2015), **55**, 1956–1965. [Google Scholar] [CrossRef]
2. Bouguettoucha, A.; Reffas, A.; Chebli, D.; Mekhalif, T.; Amrane, A. Novel activated carbon prepared from an agricultural waste, Stipa tenacissima, based on ZnCl2 activation—Characterization and application to the removal of methylene blue. Desalin. Water Treat. (2016), **57**, 24056–24069. [Google Scholar] [CrossRef]
3. Tsai, W.T.; Chang, Y.M.; Lai, C.W.; Lo, C.C. Adsorption of ethyl violet dye in aqueous solution by regenerated spent bleaching earth. J. Colloid Interface Sci.(2005), **289**, 333–338. [Google Scholar] [CrossRef]
4. Bhattacharyya, K.G.; Sharma, A. Kinetics and thermodynamics of methylene blue adsorption on neem (Azadirachta indica) leaf powder. Dye Pigment. (2005), **65**, 51–59. [Google Scholar] [CrossRef]
5. Bhattacharyya, K.G.; Sharma, A. Kinetics and thermodynamics of methylene blue adsorption on neem (Azadirachta indica) leaf powder. Dye Pigment. (2005), **65**, 51–59. [Google Scholar] [CrossRef]
6. Srinivasan, A.; Viraraghavan, T. Decolorization of dye wastewaters by biosorbents: A review. J. Environ. Manag. (2010), **91**, 1915–1929. [Google Scholar] [CrossRef]
7. Mojgan Ghanbari, Mehdi Bazarganipour, Masoud Salavati-Niasari,Photodegradation and removal of organic dyes using cui nanostructures, green synthesis and characterization,Separation and Purification Technology, Volume **173**, (2017) ,Pages 27-36,ISSN 1383-5866,https://doi.org/10.1016/j.seppur.2016.09.003.
8. Y. Chen, S.Y. Ma,Preparation and photoluminescence studies of high-quality AZO thin films grown on Zno buffered Si substrate,Materials Letters,Volume **162**, (2016),Pages 75-78,ISSN 0167-577X, https://doi.org/10.1016/j.matlet.2015.09.091.
9. Ouldmoumna, Aoumria, et al. "Characterization and application of three novel biosorbents "Eucalyptus globulus, Cynara cardunculus, and Prunus cerasefera" to dye removal." *Desalination and Water Treatment* **51**.16-18 (2013): 3527-3538.
10. Fujishima, A.; Rao, T. N.; Tryk, D. A. Titanium dioxide photocatalysis. J. Photochem. Photobiol., C (2000), 1, 1.
11. Hermana, J. M.; Guillard, C.; Disdier, J.; Lehaut, C.; Maitao, S.; Blanco, J. New industrial titania photocatalysts for the solar detoxification of water containing various pollutants. Appl. Catal., B (2002), **35**, 281.
12. Bahnermann, D. W.; Kholuiskaya, S. N.; Dillert, R.; Kulak, A. I.; Kokorin, A. Photodestruction of dichloroacetic acid catalyzed by nano-sized TiO2 particles. Appl. Catal., B (2002), **36,** 161.
13. Hoffmann, M. R.; Martin, S. T.; Choi, W.; Bahnemann, D. W. Environmental applications of semiconductor photocatalysis. Chem. Rev. (1995), **95**, 69.
14. Maeda, K. and Mallouk T.E., (2019). Two-dimensional metal oxide nanosheets as building blocks for artificial photosynthetic assemblies. Bulletin of the Chemical Society of Japan, 92(1), pp.38–54.

15. Fu, J., Xu, Q., Low, J., Jiang, C. and Yu J., (2019). Ultrathin 2D/2D WO3/g–C3N4 step-scheme H2-production photocatalyst. Applied Catalysis B Environmental, **243**, pp.556–565.
16. Roy, N., Suzuki, N., Terashima, C. and Fujishima, A., (2019). Recent improvements in the production of solar fuels: From Co2 reduction to water splitting and artificial photosynthesis. Bulletin of the Chemical Society of Japan, **92(1)**, pp.178–192.
17. Wang, Z., Li, C. and Domen, K.,(2019). Recent developments in heterogeneous photocatalysts for solar-driven overall water splitting. Chemical Society Reviews, **48(7)**, pp.2109–2125.
18. Zheng Y, Cao L, Xing G, Bai Z, Huanga J, Zhang Z (2019) Microscale fower-like magnesium oxide for highly efcient photocatalytic degradation of organic dyes in aqueous solution. RSC Adv 9:7338–7348
19. Mantilaka MMMG, De Silva RT, Ratnayake SP, Amaratunga G, de Silva KMN (2018) Photocatalytic activity of electrospun MgO nanofbres: synthesis, characterization and applications. Mater Res Bull 99:204–210
20. Aziz BK, Karim MAH (2019) Efficient catalytic photodegradation of methylene blue from medical lab wastewater using MgO nanoparticles synthesized by direct precipitation method. React Kinet Mech Catal 128:1127–1139. https://doi.org/10.1007/s11144-019-01677-8
21. Reddy, G.B.; Madhusudhan, A.; Ramakrishna, D.; Ayodhya, D.; Venkatesham, M.; Veerabhadram, G. Green Chemistry Approach for the Synthesis of Gold Nanoparticles with Gum Kondagogu: Characterization, Catalytic and Antibacterial Activity. J. Nanostruct. Chem. (2015), **5**, 185–193. [CrossRef]
22. Narath S, Koroth SK, Shankar SS, George B, Mutta V, Wacławek S, Černík M, Padil VVT, Varma RS. *Cinnamomum tamala* Leaf Extract Stabilized Zinc Oxide Nanoparticles: A Promising Photocatalyst for Methylene Blue Degradation. Nanomaterials (Basel). (2021) Jun 13;11(6):1558. doi: 10.3390/nano11061558. PMID: 34199291; PMCID: PMC8231933.